minerals

Article

Selective Flotation of Elemental Sulfur from Pressure Acid Leaching Residue of Zinc Sulfide

Guiqing Liu [1,2], Kaixi Jiang [1], Bangsheng Zhang [2], Zhonglin Dong [3,*], Fan Zhang [2], Fang Wang [2], Tao Jiang [3] and Bin Xu [3,*]

1 School of Metallurgy, Northeastern University, Shenyang 110000, China; Charles_liu32@163.com (G.L.); jiangkx@bgrimm.com (K.J.)
2 Jiangsu BGRIMM Metal Recycling Science & Technology Co. Ltd, Xuzhou 221000, China; zbsvictory@163.com (B.Z.); bkyzhangfan@126.com (F.Z.); wangfang224444@126.com (F.W.)
3 School of Minerals Processing and Bioengineering, Central South University, Changsha 410000, China; jiangtao@csu.edu.cn
* Correspondence: dongzhonglincsu@csu.edu.cn (Z.D.); xubincsu@csu.edu.cn (B.X.); Tel.: +86-183-7315-0200 (Z.D.); +86-150-8493-3770 (B.X.)

Abstract: An efficient flotation process was developed to selectively recover elemental sulfur from a high-sulfur pressure acid leaching residue of zinc sulfide concentrate. The process mineralogy analysis showed that the sulfur content reached 46.21%, and 81.97% of the sulfur existed as elemental sulfur which was the major mineral in the residue and primarily existed as pellet aggregate and biconical euhedral crystal. An elemental sulfur concentrate product with 99.9% of recovery and 83.46% of purity was obtained using the flotation process of one-time blank rougher, two-time agent-added roughers, and two-time cleaners with Z-200 as collector and Na_2S + $ZnSO_4$ + Na_2SO_3 as depressant. The flotation experiment using return water indicated that the cycle use of return water had no adverse effect on the flotation performance of elemental sulfur. The process mineralogy analysis manifested that main minerals in the residue directionally went into the flotation products. Most of elemental sulfur entered the concentrate while other minerals almost completely went into the tailing. Main valuable elements lead, zinc, and silver entered the tailing with sulfides and could be recovered by lead smelting. The proposed process can realize the comprehensive recovery of valuable components in the high-sulfur residue and thus it has wide industrial application prospect.

Keywords: high-sulfur zinc residue; elemental sulfur; process mineralogy; selective flotation; cycle use of return water

Citation: Liu, G.; Jiang, K.; Zhang, B.; Dong, Z.; Zhang, F.; Wang, F.; Jiang, T.; Xu, B. Selective Flotation of Elemental Sulfur from Pressure Acid Leaching Residue of Zinc Sulfide. *Minerals* **2021**, *11*, 89. https://doi.org/10.3390/min11010089

Received: 30 December 2020
Accepted: 13 January 2021
Published: 18 January 2021

1. Introduction

Zinc is currently the fourth most widely consumed metal in the world after iron, aluminum, and copper, and it has been widely used in automobile, machinery, battery, alloy, construction, shipping, and other industries [1,2]. Sphalerite (zinc sulfide, ZnS) is the primary mineral from which most of the world's zinc is produced [3]. Traditionally, the pyro-metallurgical process was used to treat sphalerite to obtain the zinc metal [4]. However, it is inevitable for the high-temperature route to produce toxic and hazardous flue gas containing SO_2 and heavy metals such as mercury (Hg), lead (Pb), and cadmium (Cd), which may result in serious environment problems if not treated effectively [5,6].

In order to avoid the above problem, the hydrometallurgical oxygen pressure acid leaching process was developed as an efficient route to extract zinc from sphalerite [7,8], and the leaching reaction can be expressed by the following equation:

$$ZnS + H_2SO_4 + 0.5O_2 = ZnSO_4 + H_2O + S$$

As can be seen from the equation, zinc in sphalerite is converted into soluble zinc sulfate which can be used as the raw material for recovering zinc metal by electrowinning [9].

Sulfur is oxidized into solid elemental sulfur and remains in residue [10]. Elemental sulfur is the major component of the acid leaching residue whose content can reach 40–60% [11,12]. In addition, since sphalerite is often associated with other metallic sulfides such as chalcopyrite ($CuFeS_2$), pyrite (FeS_2), and galena (PbS), thus the unreacted parts of these sulfides also enter the residue [6].

The acid leaching residue is one of the most important raw materials for recovering elemental sulfur and some other valuable elements such as silver, zinc, and lead [13,14]. As elemental sulfur has good hydrophobicity, and thus in the absence of agents, it can be effectively recovered by froth flotation, a current prevailing beneficiation technique which realizes the selective separation of target minerals from gangue minerals by making use of their natural hydrophobicity difference [15–19]. The grade of elemental sulfur in the concentrate product is generally low, mainly because of the simultaneous flotation of gangue minerals, especially the above-mentioned metallic sulfides [20]. In order to further obtain a high-purity elemental sulfur product, the hot filtration process is generally adopted after floatation [21,22]. At 115–155 °C, elemental sulfur can be effectively separated from the leaching residue by melting and filtration [23]. Unfortunately, a substantial portion of the elemental sulfur still remains in the filter cake, and its recovery is only about 60% [4,24]. A previous study showed that the elemental sulfur content in acid leaching residue needs to be greater than 70% for a high recovery by hot filtration, but this generally cannot be reached for most of the residue [25]. In addition, the valuable elements are generally scattered in elemental sulfur product and filter cake, which is unbeneficial to their subsequent recovery.

The aim of the study is to develop an efficient flotation process to selectively separate elemental sulfur from a high-sulfur pressure acid leaching residue of zinc sulfide concentrate. First, process mineralogy on the residue was studied to provide a theoretical basis for a suitable flotation process. Then, the systematic flotation experiment was performed to obtain the optimum flotation separation process. Afterwards, the flotation experiment using return water was carried out to investigate the effect of cycle use of return water on elemental sulfur recovery. Finally, process mineralogy on the concentrate and tailing was conducted to explore the distribution of concerned elements and minerals in the two flotation products.

2. Experimental

2.1. Material and Reagents

A pressure acid leaching residue of zinc sulfide concentrate from Hulun Buir Chihong Mining Industry Co., Inner Mongolia, China, was used as the raw material. The yield of the residue in the plant achieved 210,000 tons/year. The appearance of the residue shown in Figure 1 indicated that it was red-orange solid powder. The residue was dried at 70 °C for 24 h to remove its free moisture, and then it was thoroughly mixed and used for subsequent analyses and flotation experiments. All the chemical reagents used in this study were of analytical grade, and tap water was used in all experiments.

Figure 1. Appearance of the pressure acid leaching residue of zinc sulfide concentrate.

2.2. Experimental Methods

The flotation experiments of pressure acid leaching residue were performed in a self-aeration XFD-63 flotation machine [26–28]. At the beginning of the test, the residue and tap water were added into the cell and the pulp pH value was adjusted to 8.0 using lime. After that, the collector and foaming agent (methyl isobutyl carbinol, MIBC) were successively added into the pulp which was agitated at 1650 rpm for 2 min after the addition of each reagent. The aeration flotation was conducted for 5 min, and the obtained concentrate and tailing were dried and weighed for sulfur content detection to calculate sulfur recovery.

2.3. Analytical Methods

The elemental contents in solids were analyzed using acid digestion and atomic absorption spectrometer (AAS), and the elemental concentrations in solutions were measured by inductively coupled plasma-atomic emission spectrometer (ICP-AES). The sulfur phase composition in the residue was determined by using a chemical selective dissolution method which was performed based on the different dissolution behavior of sulfur phase in different solvents [16]. The particle size distribution was examined by a wet screen analysis. The mineralogical composition was ascertained by the results of chemical composition combined with X-ray diffractometer (XRD, PANalytical BV, X'Pert3 Powder, Almelo, Netherlands), Leica DMLA polarized light microscopy (Leica Corporation, Wetzla, Germany), scanning electron microscope (SEM, JSM-6360LV, JEOL, Tokyo, Japan), and energy dispersive X-ray analysis (EDAX-GENESIS, California, San Diego, USA). The embedded characteristics of samples were analyzed by the above polarized light microscopy and scanning electron microscope.

3. Results and Discussion

3.1. Process Mineralogy of High-Sulfur Residue

3.1.1. Chemical Composition and Sulfur Phase Distribution

The chemical compositions of the pressure acid leaching residue are presented in Table 1. Sulfur was the most abundant element whose content reached 46.21%, and the contents of valuable elements lead, zinc, and silver achieved 1.92%, 4.31%, and 220 g/t. Thus, this was a high-sulfur residue and possessed a high economic value. The sulfur phase analysis in Table 2 showed that 81.97% of the sulfur in the residue existed as elemental sulfur, and the remaining sulfur mainly occurred in the form of sulfide.

Table 1. Chemical compositions of the high-sulfur residue (mass fraction, %).

Element	Cu	Pb	Zn	S	Fe	SiO_2	MgO
Content	0.20	1.92	4.31	46.21	15.4	6.91	1.38
Element	Al_2O_3	CaO	As	Cd	Mn	Ag *	
Content	0.51	1.60	0.23	0.03	0.27	220.00	

* Unit g/t.

Table 2. Sulfur phase distributions of the high-sulfur residue (mass fraction, %).

Sulfur Phase	**Elemental Sulfur**	**Sulfide**	**Sulfate**	**Total**
Content	37.88	5.56	2.77	46.21
Distribution	81.97	12.03	6	100

3.1.2. Particle Size Distribution

The particle size distributions of the high-sulfur residue are shown in Table 3. The portions of particles whose size fractions were +74 and −37 um achieved 22.77% and 66.00% of the residue. Sulfur element was also mainly distributed in these two size fractions and the ratios separately reached 36.53% and 43.91%. Although the thin particle with the size fraction of −37 um had the largest sulfur distribution ratio, its sulfur grade was only 30.54%, which was evidently smaller than those (i.e. 72.07%, 83.18%, and 73.65%) of particles with the size fraction of −44~+37 um, −74~+44 um, and +74 um. This is because most of the other elements in the residue were also distributed in the size fraction of −37 um.

Table 3. Particle size distributions of the high-sulfur residue (mass fraction, %).

Size Fraction (um)	74	−74~+44	−44~+37	−37
Mass	22.77	8.06	3.17	66
S grade	73.65	83.18	72.07	30.54
S distribution ratio	36.53	14.58	4.98	43.91

3.1.3. Mineralogical Composition

The XRD spectrogram of the high-sulfur residue is shown in Figure 2, and the content of each mineral is displayed in Table 4. It can be seen that the residue had a complex mineralogical composition. Elemental sulfur was the major mineral which accounted for 37.88% of the residue. The remaining minerals could be mainly divided into four categories: sulfides (pyrite, sphalerite, and chalcopyrite), sulfates (ferric sulfate and sardinianite), oxides (quartz, massicot, and limonite), and silicates (calcium, magnesium, iron, and aluminum silicates).

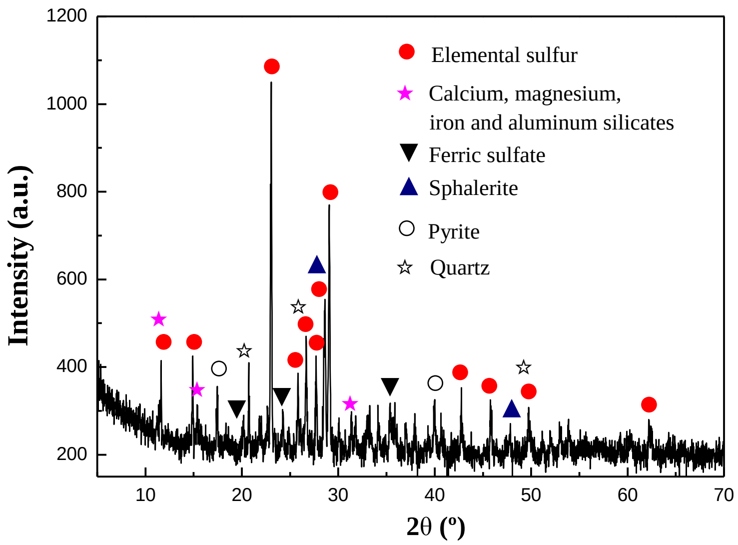

Figure 2. XRD spectrogram of the high-sulfur residue.

Table 4. Mineralogical compositions of the high-sulfur residue.

Mineral	Formula	Content (%)
Elemental sulfur	S	37.88
Ferric sulfate	$FeSO_4$	15
Pyrite	FeS_2	10
Limonite	$Fe_2O_3 \cdot 3H_2O$	10
Sphalerite	ZnS	3.5
Chalcopyrite	$CuFeS_2$	0.5
Massicot	PbO	1.8
Sardinianite	$PbSO_4$	0.2
Silicates	None	14.32
Quartz	SiO_2	2
Others	None	4.8
Total	None	100

3.1.4. Embedded Characteristic of Elemental Sulfur

Elemental sulfur was the primary mineral in the high-sulfur residue, and its embedded characteristic was analyzed and the results are shown in Figure 3a–d. From these figures, it can be concluded that elemental sulfur mainly existed as the following three forms: (1) Most of elemental sulfur existed in the form of pellet aggregate, which was generally 30–500 um in diameter (Figure 3a). A small amount of pyrite, sphalerite, and chalcopyrite were wrapped in the aggregate, and emulsion droplet chalcopyrite was found in sphalerite (Figure 3b). Elemental sulfur had estuary relation with the three metallic minerals. (2) A spot of elemental sulfur occurring as biconical autochthonous crystal with the size of 5–90 um was distributed in iron sulfate and limonite (Figure 3c). (3) Bits of 1–5 um shells of iron sulfate and limonite were observed on the surface of pellet aggregate of elemental sulfur (Figure 3d).

(a) (b) (c) (d)

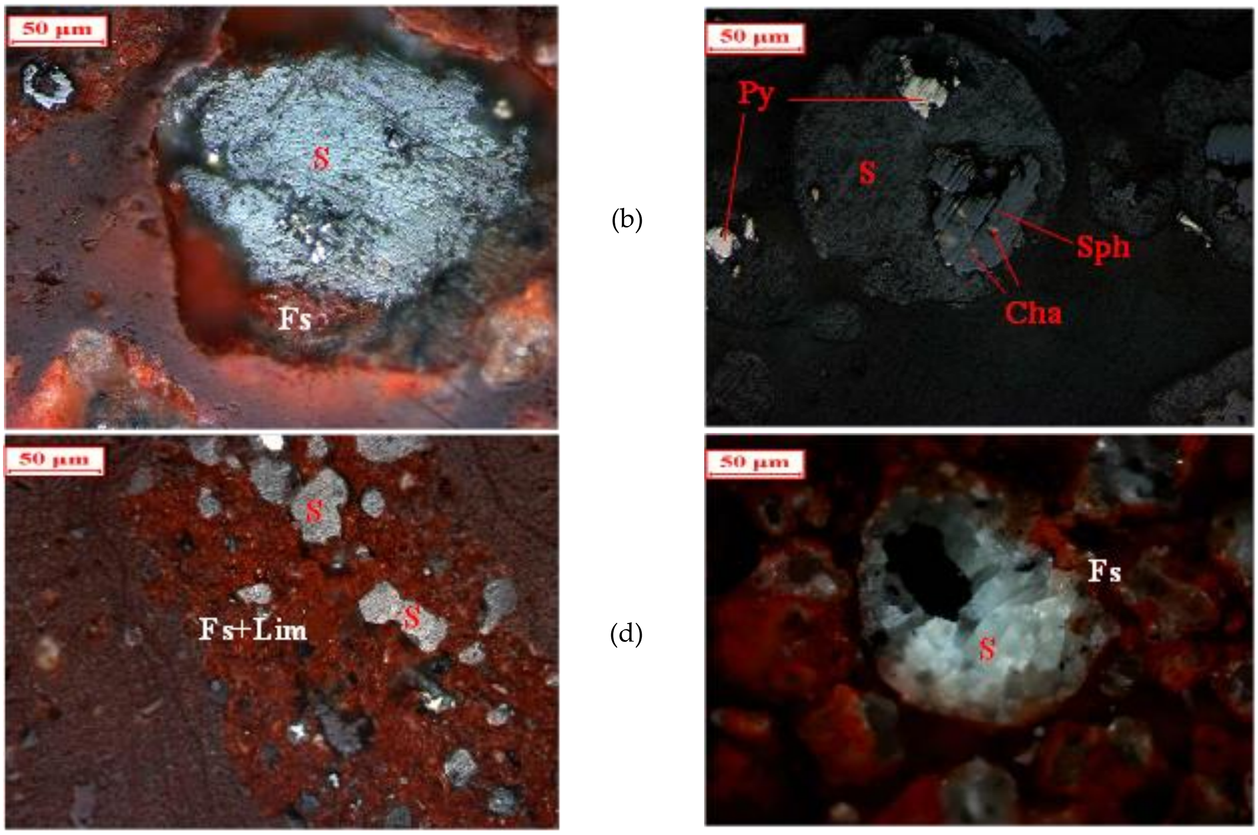

Figure 3. Embedded characteristics of elemental sulfur in the high-sulfur residue (S: elemental sulfur; Fs: ferric sulfate; Lim: limonite; Py: pyrite; Sph: sphalerite; Cha: chalcopyrite). (**a**): S and Fs (**b**): S, Py, Fs and Cha (**c**): S, Fs and Lim (**d**): S and Fs.

3.2. Flotation Experiment

3.2.1. Flotation Conditional Experiment

In order to realize the selective flotation separation of elemental sulfur from the high-sulfur residue, it is very important to select a suitable collector and depressant. Since most of the sulfur in the residue existed as elemental sulfur which has good hydrophobicity, and thus blank flotation without adding any reagents was first conducted. The obtained tailing was used for the collector selection test whose flow sheet was displayed in Figure 4a. In addition, in the following conditional experiment, the grade and recovery of total sulfur in the concentrate were considered for selecting the optimal condition because the higher the grade and recovery of total sulfur, the higher the purity and recovery of elemental sulfur.

The effect of collector type on sulfur flotation was first investigated, and the result is shown Figure 5a. When O-isopropyl-N-ethyl thionocarbamate (Z-200) (dosage: 10 g/t) was used as the collector, the sulfur recovery and its grade in the concentrate separately achieved 93.43% and 71.44%, which were larger than the results for the same dosage of three other collectors including ammonium dibutyl dithiophosphate (ADDTP), ethyl thiocarbamate (ETCM), and ethyl xanthate (EX). So, among the four collectors, Z-200 presented the optimal flotation performance for the sulfur in the high-sulfur residue.

To strengthen the separation of elemental sulfur from its gangue minerals, especially metallic sulfides, suitable depressant needs to be added to inhibit their flotation. The flow sheet is shown in Figure 4b, and the result of effect of depressant type on sulfur flotation is displayed in Figure 5b. The sulfur grade separately increased to 79.18%, 78.36%, and 78.62% when the same dosages (1000 g/t) of Na_2S, $ZnSO_4$, and Na_2SO_3 were adopted. Therefore, the use of three depressants was beneficial to improve the sulfur grade. When the mixture of three depressants (dosage: (350 + 350 + 350) g/t) was used, the grade arrived at 81.05%. So, the sulfur grade in the concentrate was further improved by the combination of the three depressants.

From the above, Z-200 and $Na_2S + ZnSO_4 + Na_2SO_3$ were the optimal collector and depressant. The effects of their dosages on sulfur flotation were investigated according to the flow sheets in Figure 4c,d, and the results are displayed in Figure 6a,b. Both the sulfur grade and recovery increased with the increase of Z-200 and $Na_2S + ZnSO_4 + Na_2SO_3$ dosages in the initial ranges of 0–10 g/t and (100 + 100 + 100) – (300 + 300 + 300) g/t. After that, the two indexes began to drop with the further increase of collector and depressant dosages. So, the optimal dosages of Z-200 and $Na_2S + ZnSO_4 + Na_2SO_3$ were 10 g/t and (300 + 300 + 300) g/t.

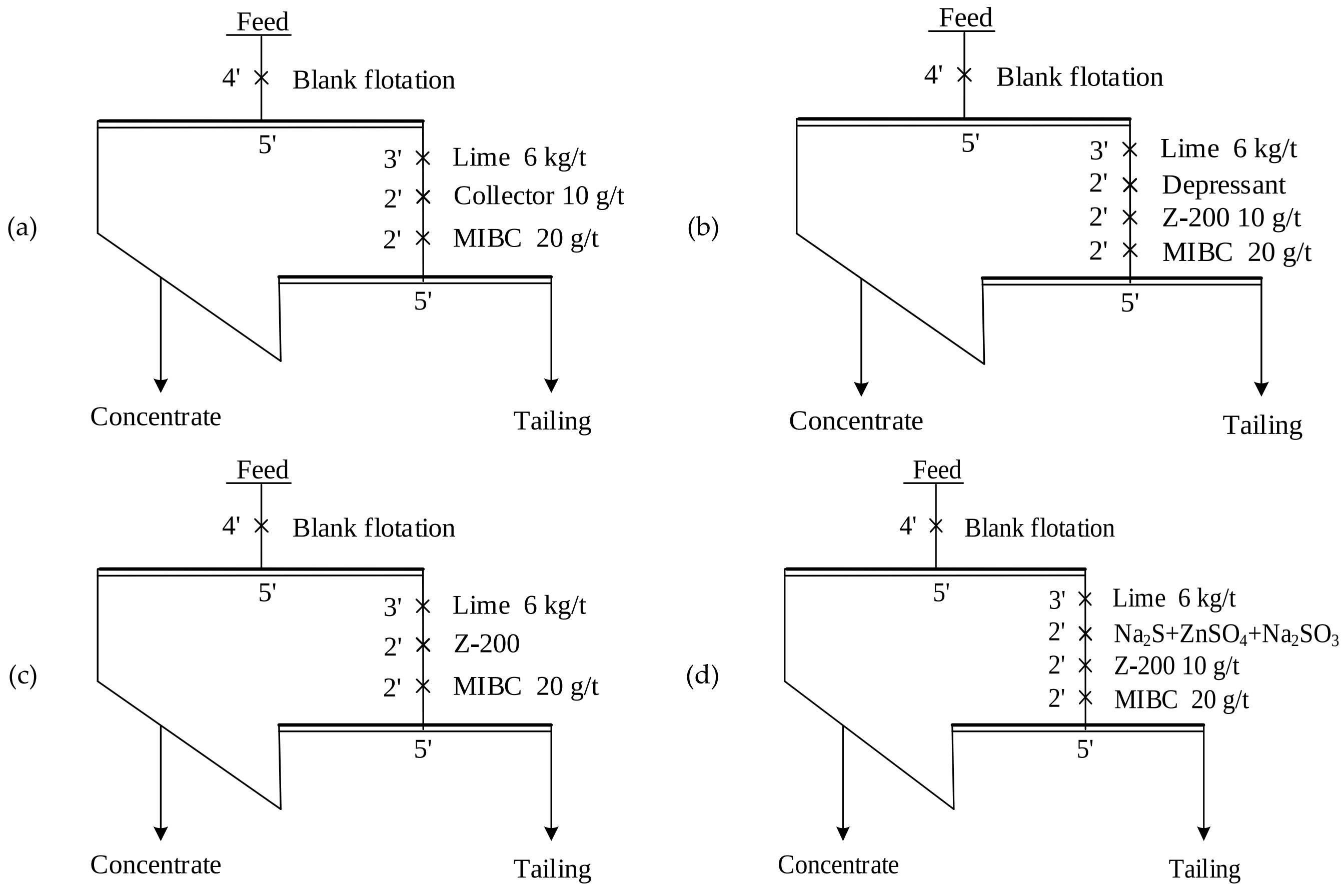

Figure 4. Flow sheets of effects of collector (**a**) and depressant (**b**) types, and Z-200 (**c**) and $Na_2S + ZnSO_4 + Na_2SO_3$ (**d**) dosages on sulfur flotation.

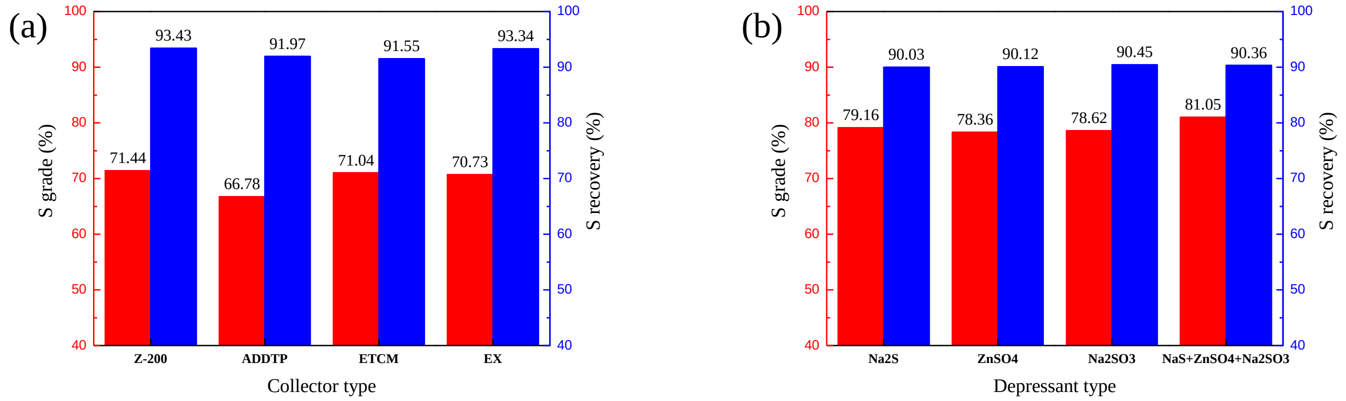

Figure 5. Effects of collector (**a**) and depressant (**b**) types on sulfur flotation. (**a**) The dosage of each collector was 10 g/t; (**b**) the dosages of single and mixed depressant were 1000 g/t and (350 + 350 + 350) g/t.

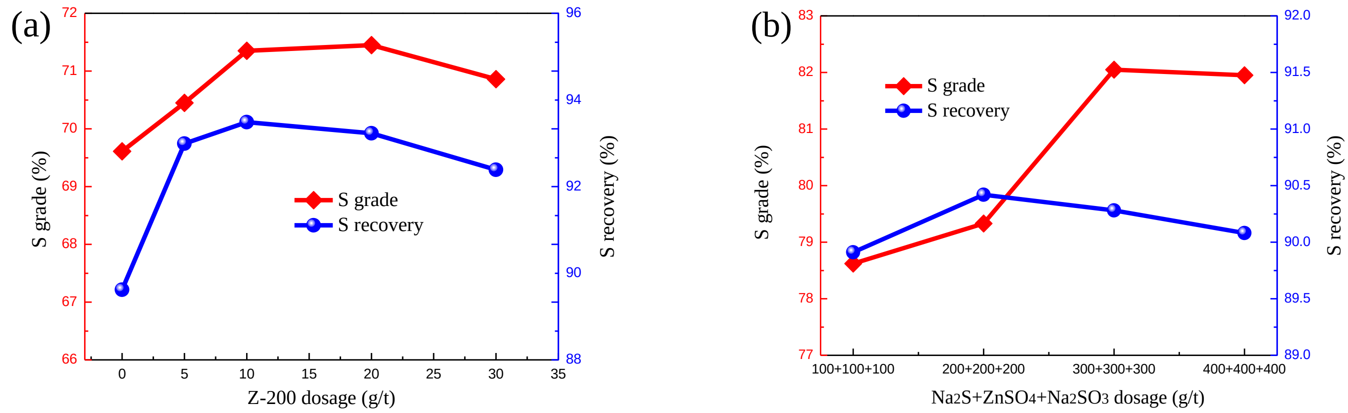

Figure 6. Effects of Z-200 (**a**) and Na_2S + $ZnSO_4$ + Na_2SO_3 (**b**) dosages on sulfur flotation.

3.2.2. Flotation Flowchart Experiment

According to the above results of flotation conditional experiment, 90.28% of the sulfur in the residue could be recovered and the sulfur grade in the obtained concentrate achieved 82.05% by using the flotation flowchart of one-time blank rougher and one-time agent-added rougher with 10 g/t Z-200 as the collector and (300 + 300 + 300) g/t Na_2S + $ZnSO_4$ + Na_2SO_3 as the depressant. In order to improve the grade and recovery, it is necessary to increase the numbers of rougher and cleaner flotation. The flow sheets of conditional experiments were displayed in Figures 7–12, and the results are shown in Tables 5 and 6.

From Table 5, it can be known that when the agent-added rougher number was two, the sulfur recovery increased to 94.16%. Further increase of agent-added rougher number did not lead to the increase of the recovery. Thus, the suitable agent-added rougher number was two. As shown in Table 6, the increase of the cleaner number effectively improved the sulfur grade. When 2-time cleaners were conducted, the sulfur grade rose to 91.88%. The grade did not evidently increase with the further increase of cleaner number. So, the optimal cleaner number was also two.

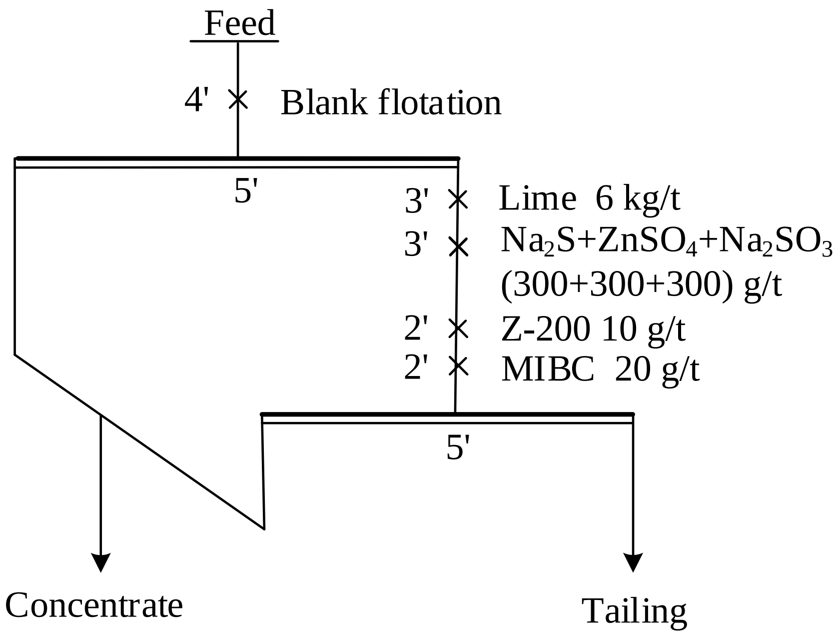

Figure 7. The flow sheet of the one-time agent-added rougher experiment.

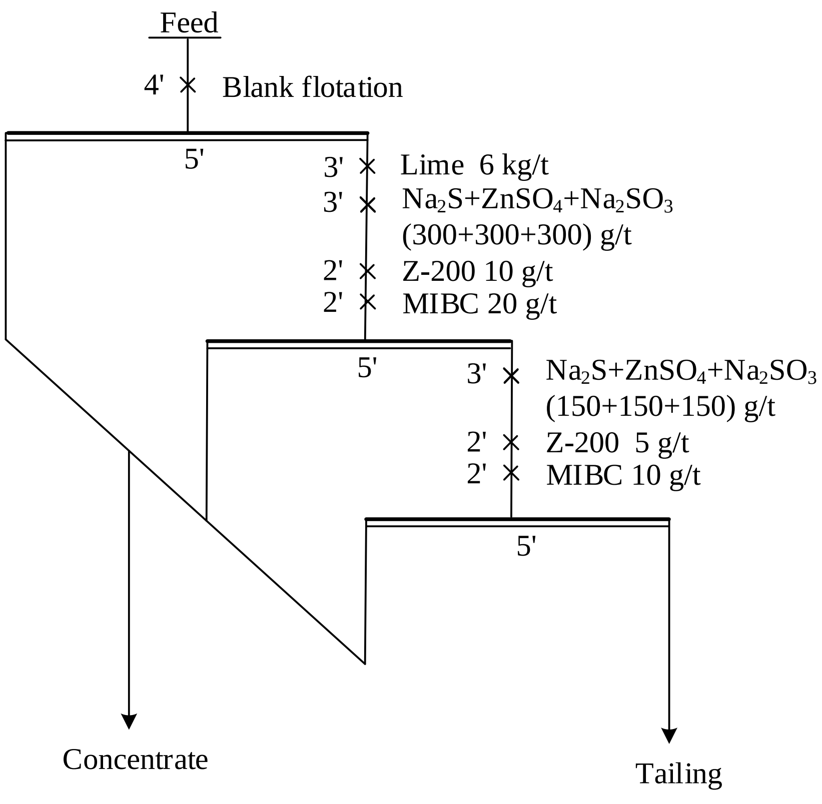

Figure 8. The flow sheet of two-time agent-added rougher experiments.

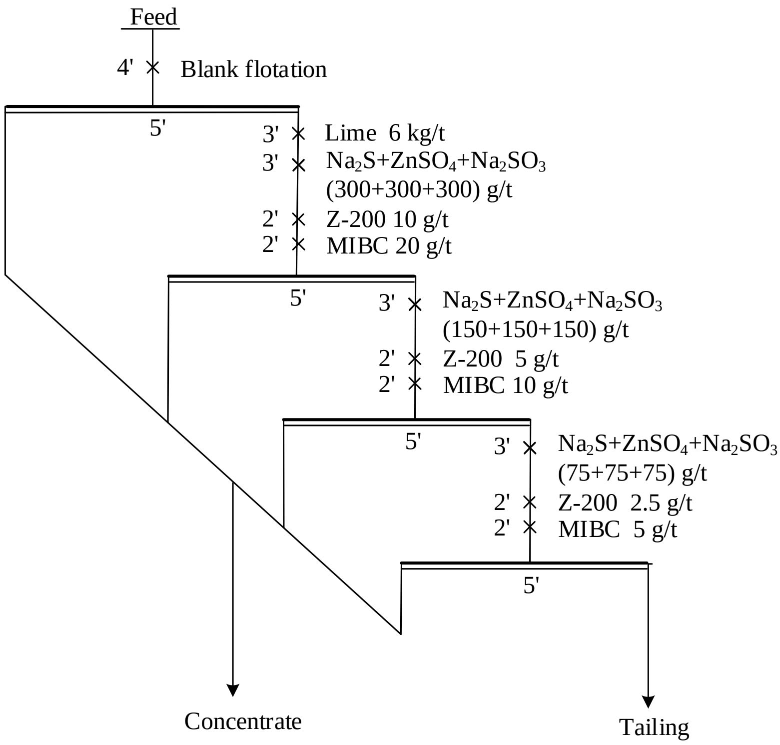

Figure 9. The flow sheet of three-time agent-added rougher experiments.

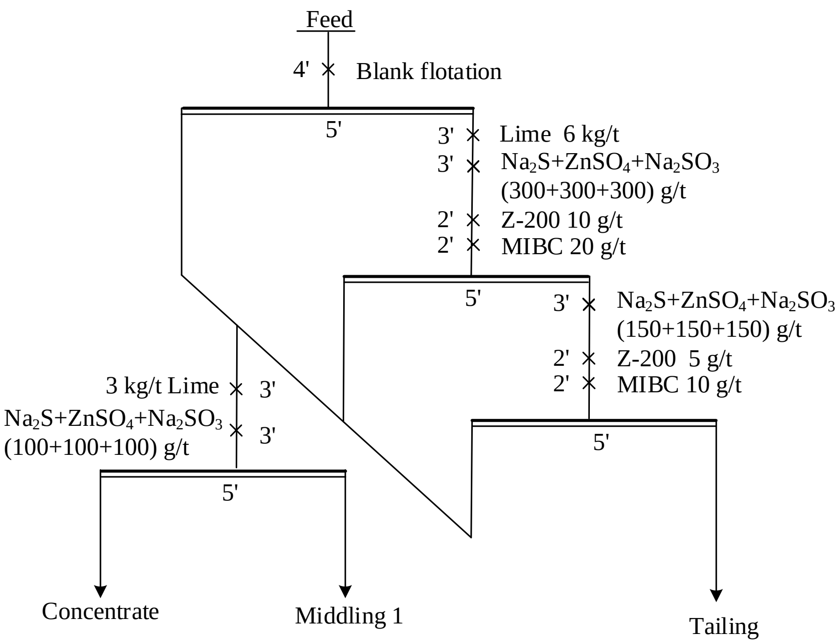

Figure 10. The flow sheet of the one-time cleaner experiment.

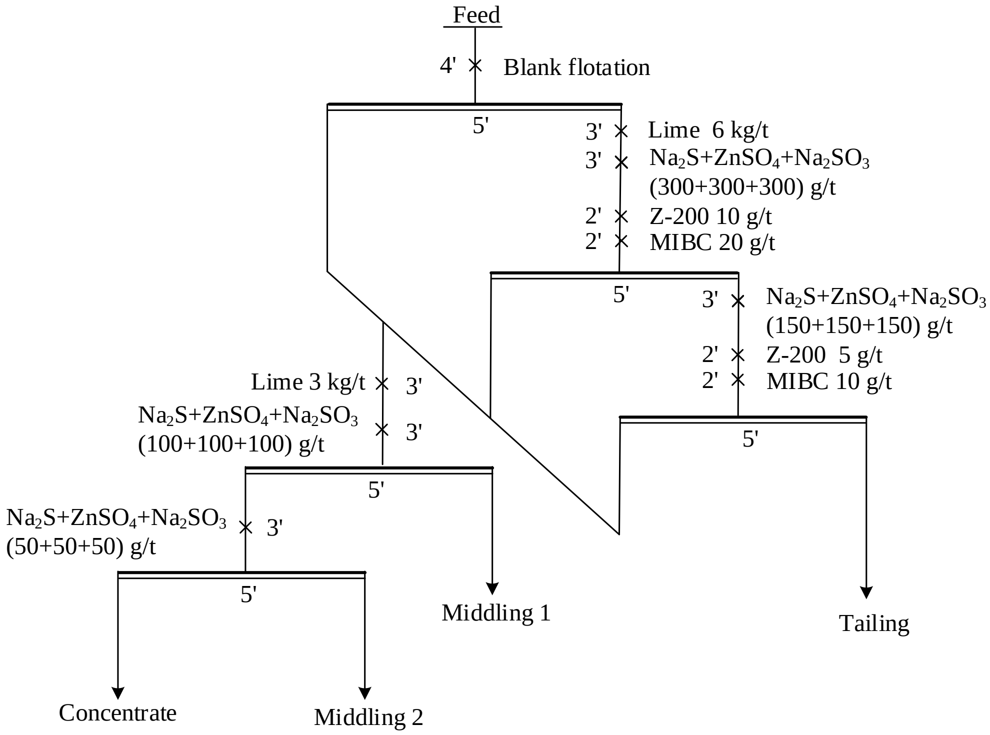

Figure 11. The flow sheet of two-time cleaner experiments.

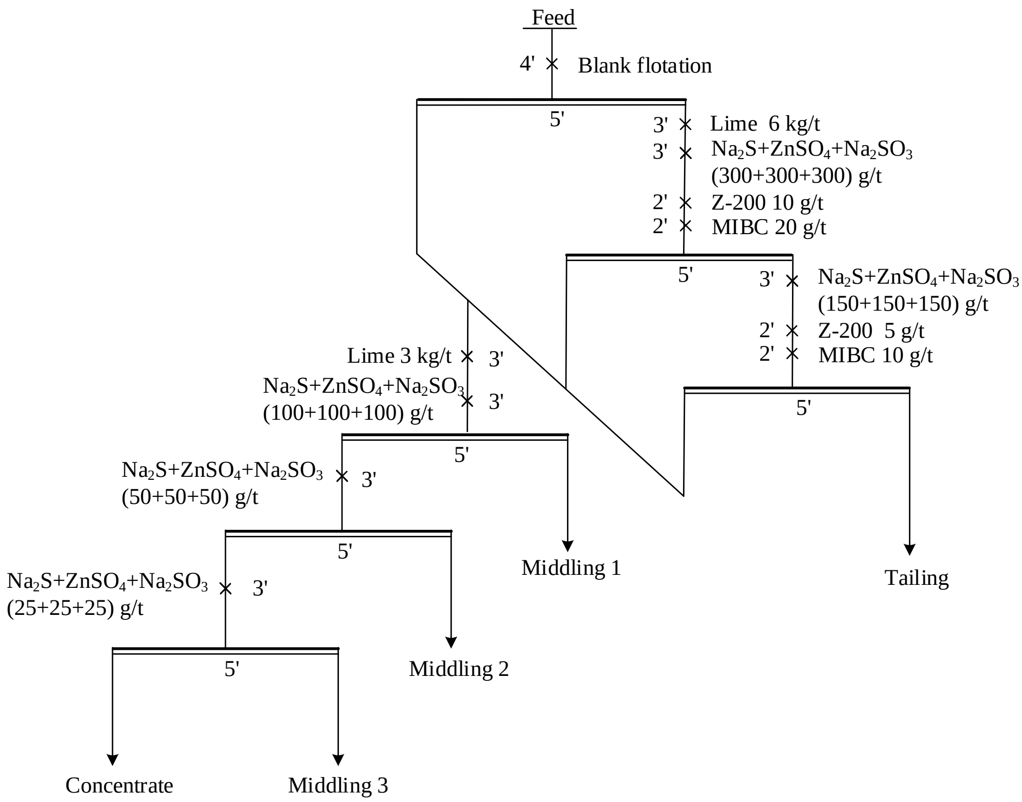

Figure 12. The flow sheet of three-time cleaner experiments.

Table 5. Effect of the agent-added rougher number on sulfur flotation.

Rougher Number	Product	Yield (%)	S Grade (%)	S Recovery (%)
1	Concentrate	50.57	82.05	90.28
	Tailing	49.43	9.07	9.72
	Feed	100.00	45.95	100.00
2	Concentrate	62.94	68.73	94.16
	Tailing	37.06	7.24	5.84
	Feed	100.00	45.94	100.00
3	Concentrate	63.30	67.56	94.01
	Tailing	36.70	7.42	5.99
	Feed	100.00	45.49	100.00

Table 6. Effect of the cleaner number on sulfur flotation.

Cleaner Number	Product	Yield (%)	S Grade (%)	S Recovery (%)
1	Concentrate	48.26	85.16	89.37
	Middling 1	17.43	13.39	5.07
	Tailing	34.31	7.44	5.55
	Feed	100.00	45.98	100.00
2	Concentrate	44.32	91.88	88.53
	Middling 1	12.75	14.45	4.01
	Middling 2	8.80	9.8	1.88
	Tailing	34.13	7.53	5.59
	Feed	100.00	45.99	100.00
3	Concentrate	44.33	92.15	89.21
	Middling 1	11.70	14.05	3.59
	Middling 2	7.44	8.98	1.46
	Middling 3	3.11	4.05	0.28
	Tailing	33.41	7.49	5.47
	Feed	100.00	45.79	100.00

3.2.3. Flotation Closed-Circuit Experiment

In order to investigate the effect of middling return on sulfur flotation, a closed-circuit flotation experiment was carried out. The flowchart is shown in Figure 13, where the tailing of the 1st cleaner (middling 1) was returned to the blank rougher, and the tailing of the 2nd cleaner (middling 2) went back to the 1st cleaner. Five-time repeated tests were conducted, and the results are listed in Table 7. It can be known from the table that after closed-circuit flotation of the high-sulfur residue, a concentrate with 91.25% of sulfur grade and 90.56% of sulfur recovery was obtained.

The quantity–quality flowchart was drawn based on the flotation results, as shown in Figure 14. The 90.56% of S, 9.27% of Zn, 6.20% of Ag, and 2.83% of Pb in the high-sulfur pressure acid leaching residue entered the concentrate. Further, 9.44% of S, 90.73% of Zn, 93.80% of Ag, and 97.17% of Pb went into the tailing. The above results indicated that S was enriched in the concentrate product while Zn, Ag, and Pb were enriched in the tailing product. For the obtained two products, the elemental sulfur concentrate can be directly sold out, and the tailing can be used as the raw material of lead smelting to further recover valuable elements Zn, Ag, and Pb.

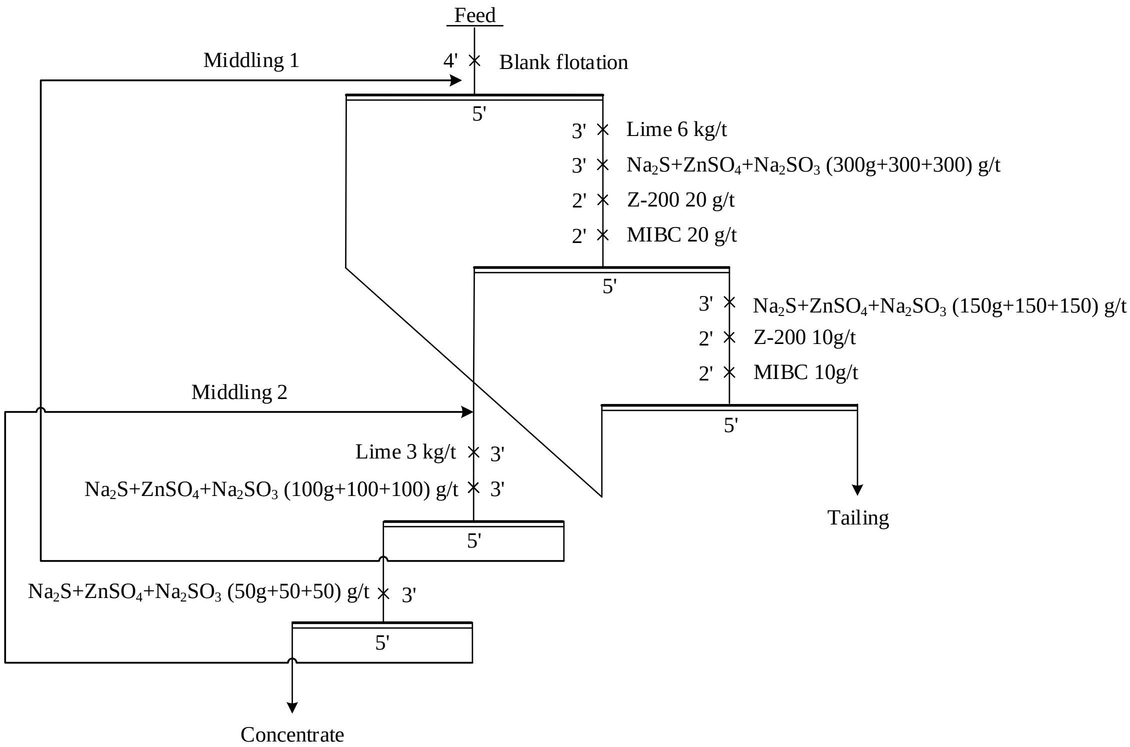

Figure 13. The flowchart of the closed-circuit flotation experiment of high-sulfur residue.

Table 7. The results of the closed-circuit flotation experiment of high-sulfur residue.

Cycle Number	Product	Yield (%)	S Grade (%)	S Recovery (%)
1	Concentrate	45.17	92.73	91.34
	Tailing	54.83	7.24	8.66
	Feed	100.00	45.86	100.00
2	Concentrate	45.48	91.73	90.71
	Tailing	54.52	7.84	9.29
	Feed	100.00	45.99	100.00
3	Concentrate	45.66	91.27	90.71
	Tailing	54.34	7.85	9.29
	Feed	100.00	45.94	100.00
4	Concentrate	45.49	91.22	90.63
	Tailing	54.51	7.87	9.37
	Feed	100.00	45.79	100.00
5	Concentrate	45.00	91.25	90.36
	Tailing	55.00	7.97	9.64
	Feed	100.00	45.45	100.00
The average result of the last three tests	Concentrate	45.38	91.25	90.56
	Tailing	54.62	7.90	9.44
	Feed	100.00	45.72	100.00

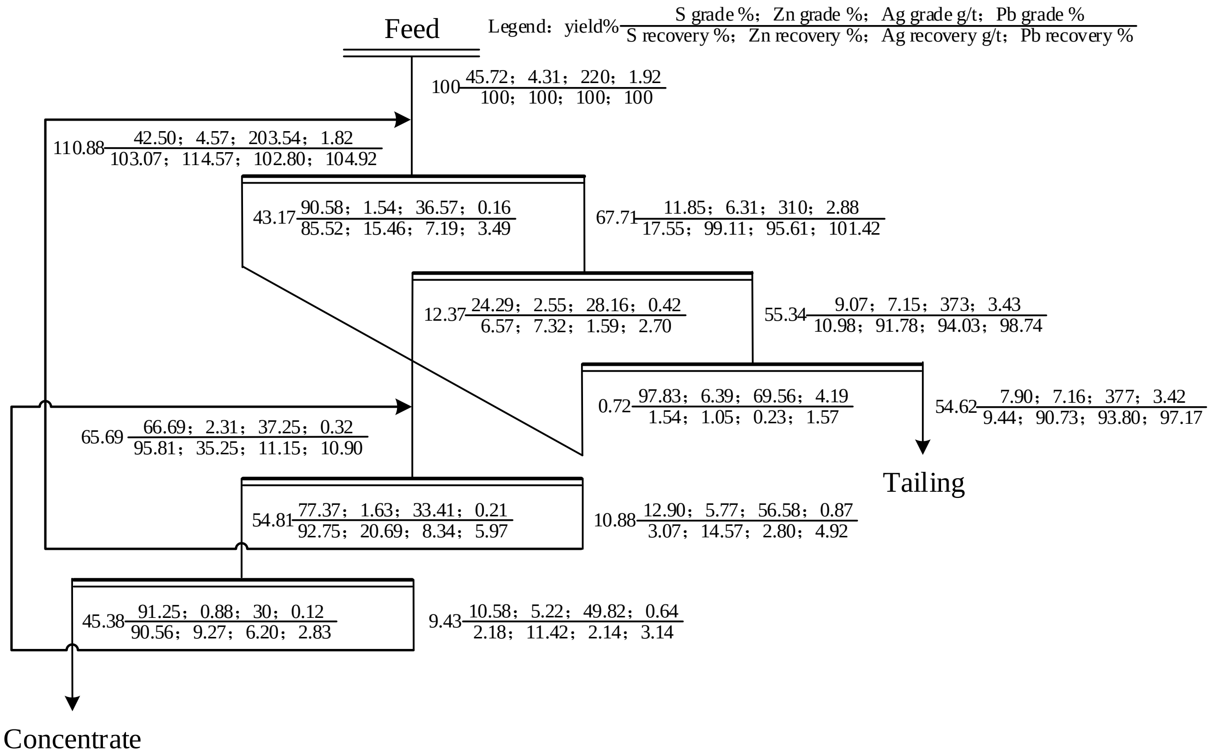

Figure 14. The quantity-quality flowchart of the closed-circuit flotation experiment of high-sulfur residue.

3.3. Cycle Use of Return Water

The cycle use of return water can not only reduce the consumption of limited freshwater resources, but also avoid the water pollution caused by the discharge of flotation wastewater [29]. Thus, the closed-circuit flotation experiment was conducted to investigate the effect of cycle use of return water on sulfur flotation. Here, five-time cycle tests were performed using the flowchart in Figure 13, where for each cycle, the filtrates of flotation concentrate and tailing are mixed and returned to the grinding and slurry mixing processes of the next cycle.

The concentration variation of each element in the filtrates of flotation concentrate and tailing with the increase of the cycle number is indicated in Tables 8 and 9. The concentrations of zinc, sulfur, calcium, sodium, and magnesium in the two filtrates increased with the cycle number in the range of 1–3, and then gradually stabilized when the cycle number was beyond three. The increased concentrations of the first four elements can be ascribed to the use of depressant while the augment of magnesium concentration may be due to the dissolution of magnesium-bearing minerals. In comparison, the variations of other elements were not obvious. The effect of cycle number of filtrates on sulfur flotation is shown in Table 10. The sulfur grade and recovery first exhibited a very slight decrease as the cycle number increased, which can be ascribed to the unfavorable impacts originating from the gradual accumulation of impurity elements in the filtrates. However, the two indexes remained at a stable high level after three cycles. Thus, the cycle use of return water did not exert obvious negative effect on sulfur flotation.

Table 8. The total element analysis results of concentrate filtrate.

Element Concentration (mg/L)	Cycle Number				
	1	**2**	**3**	**4**	**5**
Zn	265.85	532.23	797.36	799.15	796.20
S	556.33	1022.67	1459.43	1467.22	1469.00
Mg	170.67	309.00	444.58	439.97	446.30
Ca	219.60	340.20	455.23	462.77	458.80
Na	37.97	55.94	68.20	71.13	73.90
Si	3.50	3.67	3.72	3.58	3.60
K	2.90	2.82	2.78	2.92	3.00
Cd	0.16	0.15	0.13	0.12	0.12
Al	0.99	1.01	0.87	0.92	0.80
Pb	0.03	0.01	0.02	0.02	0.02
Ni	0.09	0.12	0.05	0.07	0.08
Fe	0.22	0.18	0.25	0.12	0.10

Table 9. The total element analysis results of tailing filtrate.

Element Concentration (mg/L)	Cycle Number				
	1	**2**	**3**	**4**	**5**
Zn	744.12	1487.77	2232.53	2233.95	2231.00
S	825.68	1554.56	2267.88	2279.31	2280.00
Mg	239.30	448.43	618.37	622.89	651.50
Ca	243.12	384.88	524.76	526.88	528.70
Na	40.83	62.66	80.43	81.45	82.50
Si	3.79	3.85	3.97	4.14	4.00
K	2.79	2.80	2.93	3.05	3.20
Cd	0.19	0.20	0.23	0.23	0.23
Al	1.13	1.35	1.52	1.48	1.40
Pb	0.02	0.03	0.02	0.01	0.03
Ni	0.08	0.07	0.09	0.10	0.10
Fe	0.22	0.35	0.33	0.29	0.30

Table 10. Effect of cycle number of filtrates on sulfur flotation.

Cycle Number	Product	Yield (%)	S Grade (%)	S Recovery (%)
1	Concentrate	45.41	92.33	91.28
	Tailing	54.59	7.34	8.72
	Feed	100.00	45.94	100.00
2	Concentrate	45.59	91.23	90.55
	Tailing	54.41	7.98	9.45
	Feed	100.00	45.93	100.00
3	Concentrate	45.57	91.27	90.65
	Tailing	54.43	7.88	9.35
	Feed	100.00	45.88	100.00
4	Concentrate	45.33	91.24	90.49
	Tailing	54.67	7.95	9.51
	Feed	100.00	45.71	100.00
5	Concentrate	45.69	91.25	90.67
	Tailing	54.31	7.9	9.33
	Feed	100.00	45.98	100.00

3.4. Process Mineralogy of Flotation Product

3.4.1. Chemical Composition and Sulfur Phase Distribution

After the closed-circuit flotation of the high-sulfur residue, a concentrate and a tailing were obtained and their appearances are shown in Figure 15a,b. It can be seen that these two flotation products were separately presented as light grey and red-orange powders, and their chemical compositions are displayed in Tables 11 and 12.

The sulfur content in the concentrate achieved 91.25%, which was much larger than that (i.e., 46.21%) in the leaching residue. The contents of silver, lead, and zinc were separately 30 g/t, 0.12% and 0.88%, which were evidently lower than those (i.e., 220 g/t, 1.92% and 4.31%) in the residue. In comparison, the sulfur content in the tailing was only 7.90% while the contents of silver, lead and zinc were as high as 377 g/t, 3.42% and 7.16%. Thus, it can be concluded that sulfur in the high-sulfur residue was effectively enriched in the concentrate, and the main valuable elements including silver, lead, and zinc mainly went into the tailing.

The results of sulfur phase analysis for the concentrate and tailing are displayed in Tables 13 and 14. Further, 83.46% of the sulfur in the concentrate existed as elemental sulfur, i.e., the purity of elemental sulfur concentrate product achieved 83.46%. Therefore, elemental sulfur phase primarily went into the concentrate. In comparison, only 0.13% of the sulfur in the tailing occurred as elemental sulfur, and the percentages of sulfide and sulfate separately reached 36.20% and 63.67%. Thus, sulfide and sulfate phases mainly entered the tailing.

Taking 100 kg of the high-sulfur residue as an example, the recovery of elemental sulfur was calculated as follows:

$$\text{Recovery} = (100 \times 45.38\% \times 83.46\%)/(100 \times 37.88\%) = 99.9\%.$$

The calculated result showed that 99.9% of the elemental sulfur in the high-sulfur residue was recovered using the developed closed-circuit flotation process.

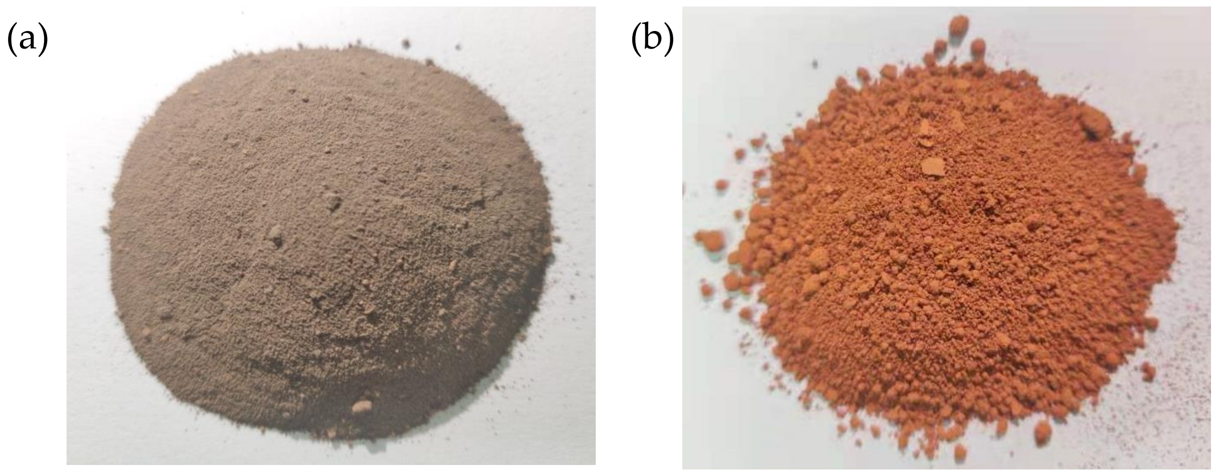

Figure 15. Appearances of the obtained flotation concentrate (**a**) and tailing (**b**) products.

Table 11. Chemical compositions of the concentrate product (mass fraction, %).

Element	Cu	Pb	Zn	S	Fe	SiO_2	MgO
Content	0.45	0.12	0.88	91.25	4.18	0.49	0.23
Element	Al_2O_3	CaO	As	Cd	Mn	Ag *	
Content	0.03	0.14	0.03	0.005	0.13	30	

* Unit g/t.

Table 12. Chemical compositions of the concentrate product (mass fraction, %).

Element	Cu	Pb	Zn	S	Fe	SiO_2	MgO
Content	0.13	3.42	7.16	7.90	27.00	13.93	0.37
Element	Al_2O_3	CaO	As	Cd	Mn	Ag *	
Content	0.01	0.38	0.39	0.05	0.17	377	

* Unit g/t.

Table 13. Sulfur phase distribution for the concentrate product (mass fraction, %).

Sulfur Phase	**Elemental Sulfur**	**Sulfide**	**Sulfate**	**Total**
Content	83.46	7.74	0.05	91.25
Distribution	91.46	8.48	0.05	100

Table 14. Sulfur phase distribution for the tailing product (mass fraction, %).

Sulfur Phase	**Elemental Sulfur**	**Sulfide**	**Sulfate**	**Total**
Content	0.01	2.86	5.03	7.9
Distribution	0.13	36.2	63.67	100

3.4.2. Particle Size Distribution

The particle size distributions of the concentrate and tailing are shown in Tables 15 and 16. The concentrate presented a scattered particle size distribution. Particularly, the particle with the size fraction of +74 um accounted for the maximum proportion (38.43%), and S distribution ratio in this fraction was also higher than those in other fractions. This may be because the elemental sulfur, the main mineral in the high-sulfur residue, agglomerated with each other during flotation and then entered the concentrate. In comparison, the particle size distribution of the tailing was concentrated. The proportion of the particle whose size fraction was −7 um achieved 97.65% while those of other fractions were very low.

Table 15. Particle size distributions of the concentrate product (mass fraction, %).

Size Fraction (um)	74	−74~+44	−44~+37	−37
Mass	38.43	31.19	7.14	23.24
S grade	91.67	95.21	87.33	86.46
S distribution ratio	38.61	32.54	6.83	22.02

Table 16. Particle size distributions of the tailing product (mass fraction, %).

Size Fraction (um)	74	−74~+44	−44~+37	−37
Mass	0.05	1.56	0.74	97.65
S grade	8.16	17.62	7.81	7.75
S distribution ratio	0.05	3.48	0.73	95.74

3.4.3. Mineralogical Composition

The XRD spectrograms of the flotation concentrate and tailing products are displayed in Figure 16a,b, and the content of each mineral is listed in Tables 17 and 18. The mineralogical compositions of the concentrate were simple, and elemental sulfur was the only detected mineral whose content arrived at 83.46%. In comparison, the mineralogical compositions of the tailing were complex. It mainly contained calcium, magnesium, iron, and aluminum silicates and ferric sulfate, small amounts of pyrite, limonite, sphalerite, and quartz, and trace amounts of elemental sulfur.

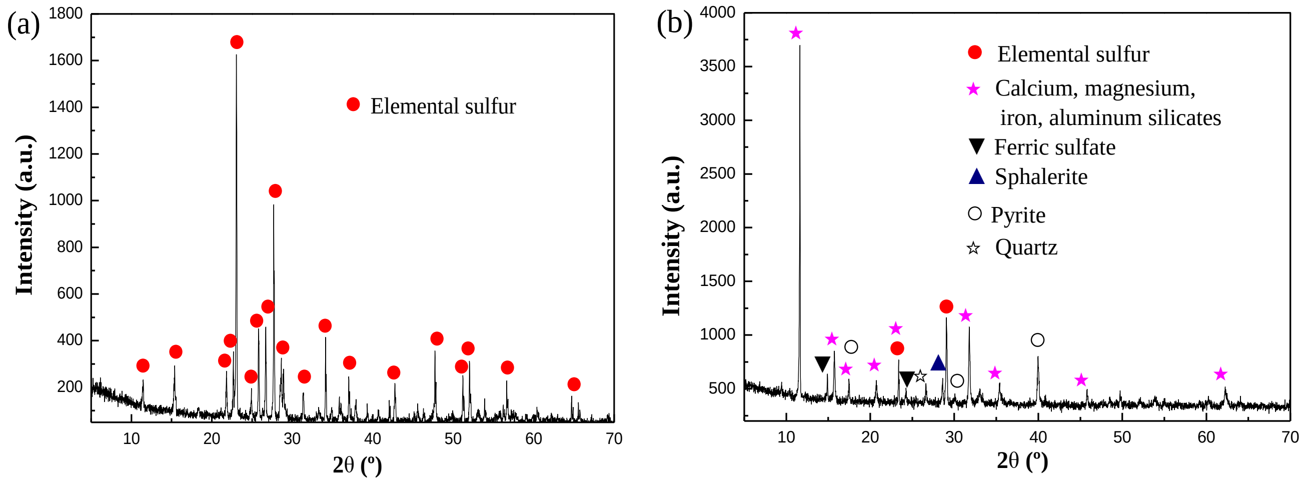

Figure 16. XRD spectrograms of the obtained concentrate (**a**) and tailing (**b**) products.

Table 17. Mineralogical compositions of the concentrate product (mass fraction, %).

Mineral	Elemental Sulfur	Ferric Sulfate	Pyrite	Limonite	Sphalerite	Chalcopyrite
Content	83.46	3.89	4.41	1.83	0.77	0.55
Mineral	Massicot	Sardinianite	Silicates	Quartz	Others	Total
Content	0.79	0.06	1.26	0.88	2.1	100

Table 18. Mineralogical compositions of the flotation tailing product (mass fraction, %).

Mineral	Elemental Sulfur	Ferric Sulfate	Pyrite	Limonite	Sphalerite	Chalcopyrite
Content	0.01	24.23	14.56	16.79	5.77	0.46
Mineral	Massicot	Sardinianite	Silicates	Quartz	Others	Total
Content	2.64	0.32	25.17	2.93	7.04	100

3.4.4. Embedded Characteristic of Flotation Products

The embedded characteristics of major minerals in the concentrate and tailing are shown in Figure 17a,b and Figure 18a–c. As indicated in Figure 17a,b, elemental sulfur, the main mineral in the concentrate, mainly existed in the form of pellet aggregate. Part of the elemental sulfur was closely associated with pyrite, sphalerite, and chalcopyrite, and these three sulfides primarily presented as irregular particles and were wrapped in the aggregate of elemental sulfur. It is difficult to separate this part of sulfides from elemental sulfur, which accounted for the presence of some sulfides in elemental sulfur concentrate. As displayed in Figure 18a–c, calcium, magnesium, iron, aluminum silicates in the tailing mainly existed in irregular columnar and granular forms. In addition, sulfides (i.e., chalcopyrite, sphalerite, and pyrite) and ferric sulfate had a close intergrowth relation. Chalcopyrite occurred in the form of emulsion droplet and was wrapped by sphalerite. Sphalerite and pyrite were embedded in ferric sulfate in disseminated or irregular granular forms. The complex embedded relationships between sulfides and between sulfides and sulfate made it difficult to separate them by flotation. Since the tailing contained high amounts of silver, lead, and zinc according to the results of chemical composition analysis in Section 3.4.1, thus it can mix with lead concentrate and be used as the raw material of lead smelting to comprehensively recover these valuable elements.

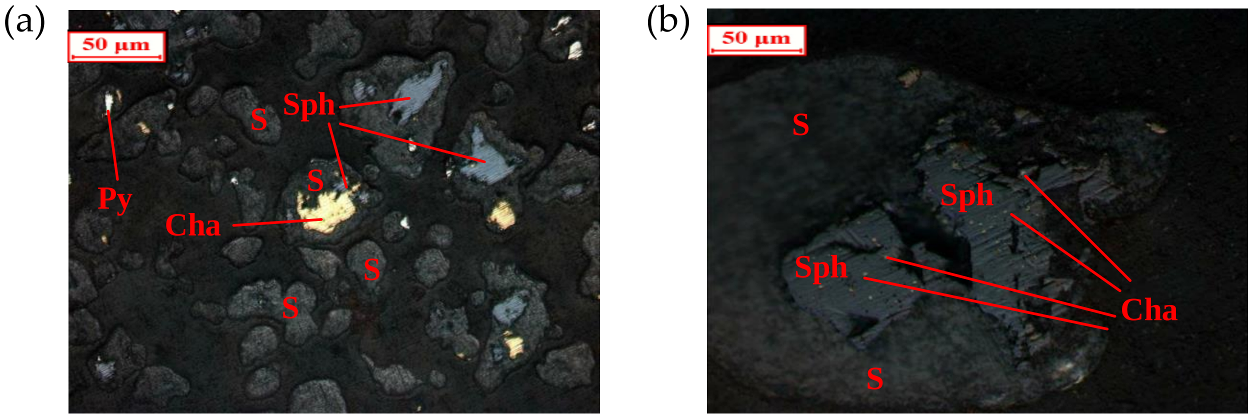

Figure 17. Embedded characteristics of major minerals in the concentrate (S: elemental sulfur; Py-pyrite; Sph: sphalerite; Cha: chalcopyrite). (**a**): S, Py, Cha and Sph (**b**): S, Cha and Sph.

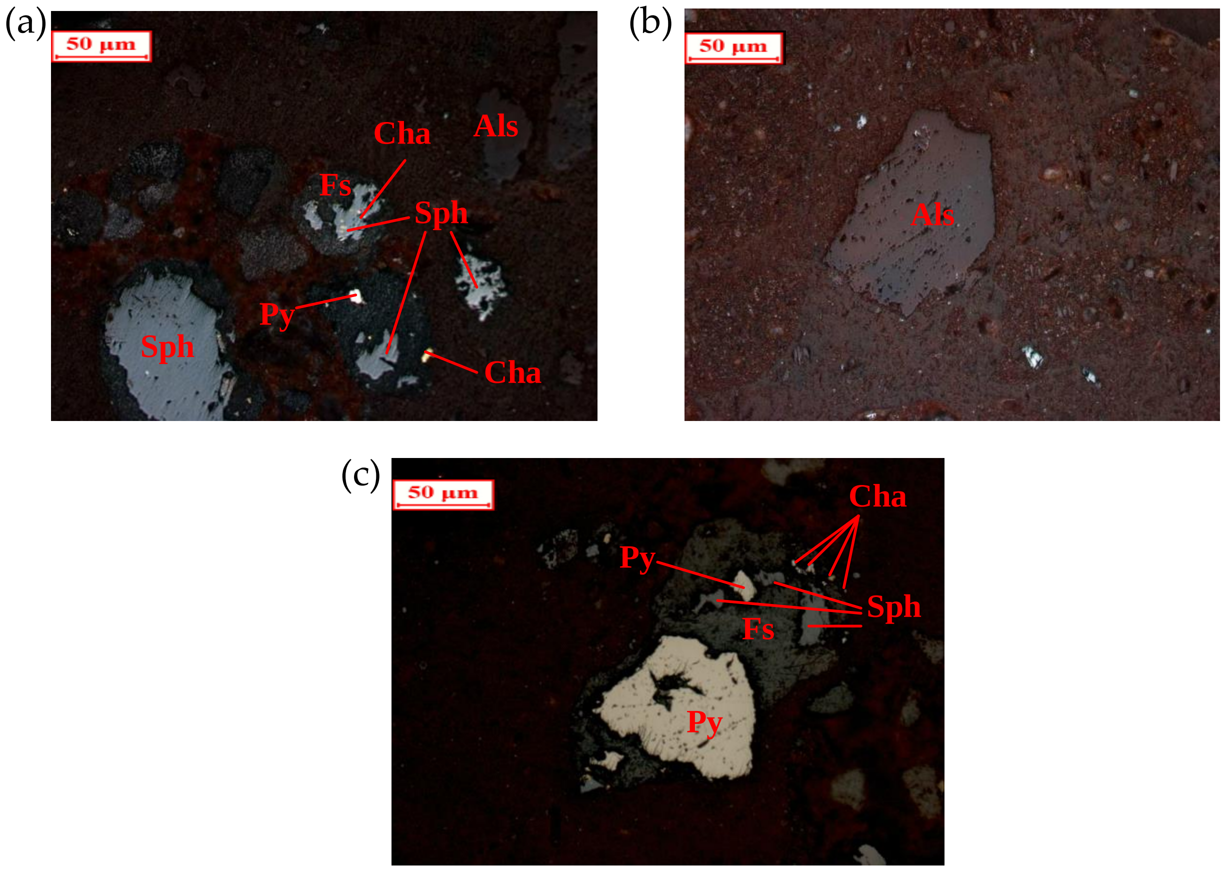

Figure 18. Embedded characteristics of major minerals in the tailing (Fs: ferric sulfate; Py-pyrite; Sph: sphalerite; Cha: chalcopyrite; Als: calcium, magnesium, iron and aluminum silicates). (**a**): Fs, Py, Cha, Als and Sph (**b**): Als (**c**): Fs, Py, Cha and Sph.

4. Conclusions

An efficient flotation process was proposed to selectively separate elemental sulfur from a high-sulfur pressure acid leaching residue of zinc sulfide concentrate. Based on the experimental results, the following conclusions can be drawn.

(1) The chemical composition and sulfur phase distribution showed that the sulfur content in the residue arrived at 46.21%, and 81.97% of the sulfur existed as elemental sulfur. The particle size distribution indicated that the portion of thin particle with the size

of -37 um achieved 66.00%, and 43.91% of sulfur in the residue was distributed in this size fraction. The mineralogical composition analysis confirmed that elemental sulfur was the major mineral in the residue whose content reached 37.88%. The embedded characteristics analysis manifested that elemental sulfur mainly existed as pellet aggregate and biconical autochthonous crystal.

(2) An efficient flotation process of one-time blank rougher, two-time agent-added roughers, and two-time cleaners with Z-200 as the collector and Na_2S + $ZnSO_4$ + Na_2SO_3 as the depressant was developed for recovering elemental sulfur in the high-sulfur residue. Under the optimal conditions, the recovery of elemental sulfur and its purity in the obtained concentrate separately reached 99.9% and 83.46%. The cycle use test of return water indicated that the concentration of major elements in the return water gradually leveled off with the increase of cycle number, and the return water still displayed a good flotation performance for elemental sulfur after 5-time cycles.

(3) The chemical composition and quantity-quality flowchart analysis indicated that the concerned elements in the high-sulfur residue were directionally distributed in the concentrate and tailing products. Further, 90.56% of S in the residue entered the concentrate while 90.73% of Zn, 93.80% of Ag, and 97.17% of Pb went into the tailing. The mineral composition and embedded characteristic analysis manifested that the directional distribution of main minerals in the residue was also realized. Elemental sulfur occurring as pellet aggregate entered the concentrate, while silicates existing in irregular columnar and granular forms, and sulfides and sulfates presenting close intergrowth went into the tailing.

Author Contributions: Conceptualization, Z.D., B.X. and T.J.; methodology, G.L., B.Z. and K.J.; software, F.Z.; validation, T.J.; formal analysis, F.W.; investigation, G.L.; resources, G.L.; data curation, Z.D.; writing—original draft preparation, G.L. and Z.D.; writing—review and editing, Z.D. and B.X.; supervision, B.X. and T.J.; funding acquisition, G.L. All authors have read and agreed to the published version of the manuscript.

Funding: This research was funded by National Key Research and Development Program of China (No. 2018YFC1902006).

Institutional Review Board Statement: Not applicable.

Informed Consent Statement: Not applicable.

Data Availability Statement: Data available in a publicly accessible repository.

Conflicts of Interest: The authors declare no conflict of interest.

References

1. Dong, Z.L.; Jiang, T.; Xu, B.; Yang, Y.B.; Li, Q. An eco-friendly and efficient process of low potential thiosulfate leaching-resin adsorption recovery for extracting gold from a roasted gold concentrate. *J. Clean. Prod.* **2019**, *229*, 387–398. [CrossRef]
2. Dong, Z.L.; Jiang, T.; Xu, B.; Yang, J.K.; Chen, Y.Z.; Yang, Y.B.; Li, Q. Comprehensive recoveries of selenium, copper, gold, silver and lead from a copper anode slime with a clean and economical hydrometallurgical process. *Chem. Eng. J.* **2020**, *393*, 124762. [CrossRef]
3. Gu, Y.; Zhang, T.A.; Liu, Y.; Mu, W.Z.; Zhang, W.G.; Dou, Z.H.; Jiang, X.L. Pressure acid leaching of zinc sulfide concentrate. *Trans. Nonferrous Met. Soc. China* **2010**, *20*, s136–s140. [CrossRef]
4. Li, H.L.; Wu, X.Y.; Wang, M.X.; Wang, J.; Wu, S.K.; Yao, X.L.; Li, L.Q. Separation of elemental sulfur from zinc concentrate direct leaching residue by vacuum distillation. *Sep. Purif. Technol.* **2014**, *138*, 41–46. [CrossRef]
5. Padilla, R.; Vega, D.; Ruiz, M.C. Pressure leaching of sulfidized chalcopyrite in sulfuric acid–oxygen media. *Hydrometallurgy* **2010**, *86*, 80–88. [CrossRef]
6. Liu, F.P.; Wang, J.L.; Peng, C.; Liu, Z.H.; Wilson, B.P.; Lundström, M. Recovery and separation of silver and mercury from hazardous zinc refinery residues produced by zinc oxygen pressure leaching. *Hydrometallurgy* **2019**, *185*, 38–45. [CrossRef]
7. Qin, S.C.; Jiang, K.X.; Wang, H.B.; Zhang, B.S.; Wang, Y.F.; Zhang, X.D. Research on behavior of iron in the zinc sulfide pressure leaching process. *Minerals* **2020**, *10*, 224–239. [CrossRef]
8. Rao, S.; Wang, D.X.; Liu, Z.Q.; Zhang, K.F.; Cao, H.Y.; Tao, J.Z. Selective extraction of zinc, gallium, and germanium from zinc refinery residue using two stage acid and alkaline leaching. *Hydrometallurgy* **2019**, *183*, 38–44. [CrossRef]
9. Dong, Z.L.; Jiang, T.; Xu, B.; Yang, Y.B.; Li, Q. Recovery of gold from pregnant thiosulfate solutions by the resin adsorption technique. *Metals* **2017**, *7*, 555–572. [CrossRef]

10. Ozberk, E.; Jankola, W.A.; Vecchiarelli, M.; Krysa, B.D. Commercial operations of the Sherritt zinc pressure leach process. *Hydrometallurgy* **1995**, *39*, 49–52. [CrossRef]
11. Xu, B.; Yang, Y.B.; Li, Q.; Jiang, T.; Li, G.H. Stage leaching of a complex polymetallic sulfide concentrate: Focus on the extraction of Ag and Au. *Hydrometallurgy* **2016**, *159*, 87–94. [CrossRef]
12. Xu, B.; Yang, Y.B.; Li, Q.; Yin, W.; Jiang, T.; Li, G.H. Thiosulfate leaching of Au, Ag and Pd from a high Sn, Pb and Sb bearing decopperized anode slime. *Hydrometallurgy* **2016**, *164*, 278–287. [CrossRef]
13. Fan, Y.Y.; Liu, Y.; Niu, L.P.; Jing, T.L.; Zhang, T.A. Separation and purification of elemental sulfur from sphalerite concentrate direct leaching residue by liquid paraffin. *Hydrometallurgy* **2019**, *186*, 162–169. [CrossRef]
14. Wang, Z.Y.; Cai, X.L.; Zhang, Z.B.; Zhang, L.B.; Wang, S.X.; Peng, J.H. Separation and enrichment of elemental sulfur and mercury from hydrometallurgical zinc residue using sodium sulfide. *Trans. Nonferrous Met. Soc. China* **2015**, *25*, 640–646. [CrossRef]
15. Huang, Z.Q.; Zhong, H.; Wang, S.; Xia, L.Y.; Zou, W.B.; Liu, G.Y. Investigations on reverse cationic flotation of iron ore by using a Gemini surfactant: Ethane-1,2-bis (dimethyl-dodecyl-ammonium bromide). *Chem. Eng. J.* **2014**, *257*, 218–228. [CrossRef]
16. Wang, Z.; Xu, L.H.; Wang, J.M.; Wang, L.; Xiao, J.H. A comparison study of adsorption of benzohydroxamic acid and amyl xanthate on smithsonite with dodecylamine as co-collector. *Appl. Surf. Sci.* **2017**, *426*, 1141–1147. [CrossRef]
17. Xing, P.; Ma, B.Z.; Wang, C.Y.; Wang, L.; Chen, Y.Q. A simple and effective process for recycling zinc-rich paint residue. *Waste Manag.* **2018**, *76*, 234–241. [CrossRef]
18. Xu, B.; Yang, Y.B.; Li, Q.; Jiang, T.; Zhang, X.; Li, G.H. Effect of common associated sulfide minerals on thiosulfate leaching of gold and the role of humic acid additive. *Hydrometallurgy* **2017**, *171*, 44–52. [CrossRef]
19. Xu, B.; Kong, W.H.; Li, Q.; Yang, Y.B.; Jiang, T. A review of thiosulfate leaching of gold: Focus on thiosulfate consumption and gold recovery from pregnant solution. *Metals* **2017**, *7*, 222–237. [CrossRef]
20. Xu, B.; Li, K.; Zhong, Q.; Li, Q.; Yang, Y.B.; Jiang, T. Study on the oxygen pressure alkali leaching of gold with generated thiosulfate from sulfur oxidation. *Hydrometallurgy* **2018**, *177*, 178–186. [CrossRef]
21. Xu, B.; Li, K.; Dong, Z.L.; Yang, Y.B.; Li, Q.; Liu, X.L.; Jiang, T. Eco-friendly and economical gold extraction by nickel catalyzed ammoniacal thiosulfate leaching-resin adsorption recovery. *J. Clean. Prod.* **2019**, *233*, 1475–1485. [CrossRef]
22. Xu, B.; Li, K.; Li, Q.; Yang, Y.B.; Liu, X.L.; Jiang, T. Kinetic studies of gold leaching from a gold concentrate calcine by thiosulfate with cobalt-ammonia catalysis and gold recovery by resin adsorption from its pregnant solution. *Sep. Purif. Technol.* **2019**, *213*, 368–377. [CrossRef]
23. Xu, B.; Chen, Y.Z.; Dong, Z.L.; Jiang, T.; Zhang, B.S.; Liu, G.Q.; Yang, J.K.; Li, Q.; Yang, Y.B. Eco-friendly and efficient extraction of valuable elements from copper anode mud using an integrated pyro-hydrometallurgical process. *Resour. Conserv. Recycl.* **2021**, *164*, 105195. [CrossRef]
24. Li, H.L.; Yao, X.L.; Wang, M.X.; Wu, S.K.; Ma, W.W.; Wei, W.W.; Li, L.Q. Recovery of elemental sulfur from zinc concentrate direct leaching residue using atmospheric distillation: A pilot-scale experimental study. *J. Air Waste Manag.* **2014**, *64*, 95–103. [CrossRef] [PubMed]
25. Halfyard, J.E.; Hawboldt, K. Separation of elemental sulfur from hydrometallurgical residue: A review. *Hydrometallurgy* **2011**, *109*, 80–89. [CrossRef]
26. Jia, Y.; Huang, K.H.; Wang, S.; Cao, Z.F.; Zhong, H. The selective flotation behavior and adsorption mechanism of thiohexanamide to chalcopyrite. *Miner. Eng.* **2019**, *137*, 187–199. [CrossRef]
27. Jia, Y.; Huang, X.P.; Cao, Z.F.; Wang, S.; Zhong, H. Investigation on the selectivity of thioamide surfactants and adsorption mechanism of thio-p-toluamide for chalcopyrite. *Appl. Surf. Sci.* **2019**, *484*, 864–875. [CrossRef]
28. Zhao, K.L.; Gu, G.H.; Yan, W.; Wang, X.H.; Wang, C.Q.; Xu, L.H. Flotation of fine pyrite by using N-dodecyl mercaptan as collector in natural pH pulp. *J. Mater. Res. Technol.* **2019**, *8*, 1571–1575. [CrossRef]
29. Muzind, I.; Schreithofer, N. Water quality effects on flotation: Impacts and control of residual xanthates. *Miner. Eng.* **2018**, *125*, 34–41. [CrossRef]